LA-13902-MS

Approved for public release;
distribution is unlimited.

Measurement of the Inclusive Cross Sections for Production of ^{7}Be and ^{22}Na by 800 MeV Protons on ^{23}Na

Los Alamos National Laboratory is operated by the University of California for the United States Department of Energy under contract W-7405-ENG-36.

An Affirmative Action/Equal Opportunity Employer

LA-13902-MS

Issued: February 2002

Measurement of the Inclusive Cross Sections for Production of ^{7}Be and ^{22}Na by 800 MeV Protons on ^{23}Na

*Raymond T. Klann**
George L. Morgan
Keith A. Woloshun

**Argonne National Laboratory, 9700 S. Cass Avenue, Argonne, IL 60439.*

Los Alamos
NATIONAL LABORATORY

Los Alamos NM 87545

Measurement of the inclusive cross sections for production of ^{7}Be and ^{22}Na by 800 MeV protons on ^{23}Na

Raymond T. Klann
Argonne National Laboratory

George L. Morgan and Keith A. Woloshun
Los Alamos National Laboratory

Abstract

Measurements have been made of the total cross sections for the production of ^{7}Be and ^{22}Na from sodium metal bombarded by 800 MeV protons. A large Ge detector was used to count the gamma rays from disintegration of these isotopes in thin samples of sodium after irradiation by protons from the LANSCE accelerator. The results are compared to isotope production calculated using the MCNPX code system.

Introduction

Sodium cooled target assemblies are under consideration for various Advanced Accelerator Applications (AAA). The inventory of radioactive isotopes in such assemblies will be driven in part by the activation of the sodium coolant by direct or scattered protons of the accelerator beam. Such activities are calculated for various target designs using high-energy transport codes. These codes calculate the production of these isotopes using various physics models to estimate the interaction of high-energy particles with target materials. Measurement of the production of radioactive isotopes provides a way to test the efficacy of such simulations. Bombardment of sodium by high energy protons can produce several isotopes with half-lives longer than an hour. These include ^{22}Na, ^{14}C, ^{7}Be, and ^{3}H. The ^{22}Na and ^{7}Be isotopes decay with the emission of easily detected gamma rays and thus their cross sections can be readily determined from irradiated samples. The other isotopes decay by beta emission and can only be detected through more complicated processing of the sample. We have used the technique of gamma ray counting to determine the cross sections for production of ^{22}Na and ^{7}Be by the irradiation of sodium samples with 800 MeV protons.

Sample Preparation

Samples of sodium metal were contained in thin (0.025 cm) stainless steel cans. These samples were 0.5 cm thick with a diameter of 7.62 cm. A primary consideration in deciding the sample thickness is to insure that neutron production in the sample does not contribute appreciably to the production of the isotopes of interest. Calculations with the code MCNPX [1] were used to estimate this effect and indicated that for the thickness chosen here, the neutron production was negligible.

The sample holders were fabricated from stainless steel tubing with an outer diameter of 7.62 cm (wall thickness of 0.165 cm). The inner diameter of the tubing was 7.29 cm. The tubing was cut to a height of 0.5 cm. Two opposing holes were drilled in the side of the tubing to allow fill lines (0.476 cm diameter) to be welded to the tubing. Stainless steel sheet (thickness of 0.025 cm) was seal welded onto the top and bottom surfaces – leaving an empty stainless steel disk for filling with sodium using the two filling lines.

Metallic sodium was purchased from Fisher Scientific Company. A chemical analysis for the sodium was provided and is listed in Table 1.

Table 1
Analysis results for sodium

Description	Specifications	Test Result
Appearance	Soft, silvery metal	Silvery metallic bar
Chloride	0.002% maximum	<0.0020%
Heavy Metals	5 ppm maximum	<5.00 ppm
Identification	Pass/fail	Pass
Iron	0.001% maximum	<0.00100%
Nitrogen Compounds	0.003% maximum	<0.0030%
Phosphate	5 ppm maximum	5.000 ppm
Sulfate	0.002% maximum	<0.0020%

The sample holders and metallic sodium were then transferred to an argon-atmosphere glovebox for filling. All operations except seal welding and quality checks were performed in the glovebox. Two reservoirs with surface heating and a furnace were used to fill the disks with sodium, forming three separate heated zones. One reservoir was filled with solid sodium and the other reservoir served as the overflow reservoir to verify that the disk was filled.

The procedure for filling the disks was to pre-heat the overflow reservoir and furnace to 200° C, then begin to heat the supply reservoir to melt the solid sodium. The temperature was selected to improve viscosity effects without making the operation time consuming. As the sodium melted, it flowed into the disk from gravity and filled the disk from the bottom (the inlet tubing was at the lowest point in the system). The operation continued until the overflow reservoir was partially filled with sodium. A hand pump was then used to provide headspace pressure in the reservoirs (on an alternating basis) to force a small flow in the sodium lines. The heat was then removed from the fill reservoir, and it was allowed to cool and solidify. The furnace was then shut off to begin slowly cooling the sample from the bottom up. The overflow reservoir and tubing were maintained at 200° C to allow sodium to feed into the sample from the top to account for the change in density.

The sodium undergoes three density changes during cooling. When the sodium is molten, it cools from 200° C to 100° C and undergoes a 2.5% density change. As the sodium undergoes a phase change from liquid to solid, it undergoes another density change of 2.7%. Sodium from the overflow reservoir fills the void space caused by the shrinkage. The heat is removed from the overflow reservoir, and the entire system is allowed to cool.

After cooling, the VCR connectors were disassembled, and the VCR fittings were cut from the tubing at 3.81 cm from the disk. The tubing was then excavated to remove sodium and crimped about 1.25 cm from the disk. A second crimp was then placed at the end of the tubing to initially seal the tube. The disk was then removed from the glovebox, and the tubing ends seal welded. The disks were then radiographed to verify that there were no void spaces in the samples.

Experimental Procedure

A schematic diagram of the experimental configuration is shown in Figure 1. A photograph of the sample is shown in Figure 2. The proton beam was provided by the LANSCE accelerator at the Los Alamos National Laboratory. The proton beam exited the beam line vacuum through a thin stainless steel window, traveled about 2 meters through air, and then was incident on the sample. An identical sample was located near the primary sample but out of the proton beam. The activation of this sample was used as a measure of isotope production by neutrons and/or scattered protons. A second irradiation was carried in a similar configuration using empty stainless steel containers to determine the production of the isotopes of interest in the container. Each irradiation lasted about one hour with a proton beam current of about 30 nanoamperes. After irradiation, the samples were removed from the target cave and stored for about one week to allow the shorter-lived background activities to decay away.

A primary requirement for the measurement of proton activation is the determination of the parameters of the incident beam. These parameters include the total integrated beam striking the target assembly in each irradiation, the position of the beam on the target, and the beam intensity profile. The beam monitor system is shown schematically in Figure 1.

The incident beam current was monitored in the LAMPF Central Control Room using a standard LAMPF current monitor [2] located in the proton beam line about three meters upstream from the target. A digital reading from this monitor was recorded at 1 second intervals over the course of each irradiation, and the file of current values so generated was used to document the time dependence of the current and, from its integral, to determine the total number of protons incident on the sample for a given irradiation. The systematic uncertainty in the calibration of this beam monitor is estimated to be about 3%. The monitor reads out with a precision of 1 nanoamp. The nominal current used in this work was about 30 nanoamps, so this adds a second uncertainty of about 3% for an overall uncertainty of about 4.5%.

A second method employing an aluminum activation foil was also used to determine the integrated proton fluence on the target assembly for each irradiation. The method employed a

stack of three aluminum foils, each nominally 0.32 mm in thickness. The exact thickness of each foil was determined by weighing the foil and carefully measuring its dimensions (nominally 10 by 10 cm). Thickness measurements with a micrometer were also used to test the uniformity. Variations over the foil were found to be negligible. The proton beam fluence was then determined by counting the ^{24}Na activation products using a Germanium gamma-ray detector. Only the middle foil in each stack was counted; the presence of the upstream and downstream foils was to insure that the center foil was in equilibrium with any recoiling reaction products. The cross section for production of ^{24}Na by 800 MeV protons has been studied carefully in Ref. 3 and has an uncertainty of less than 2%. The half-life for ^{24}Na is 14.9590 hours, and the 1.368 MeV gamma ray is produced in 99.9936% of the decays. A calibrated ^{60}Co source was counted simultaneously with the aluminum foil. In this way the activity of the ^{24}Na could be determined by direct comparison of the counting rate with ^{60}Co source, requiring only a small correction for the difference in energies between the 1.332 MeV gamma ray from ^{60}Co and the 1.368 MeV gamma ray from ^{24}Na. The ^{60}Co source was NIST traceable with quoted uncertainties of 2% (at the 99% confidence level). The measured activity was corrected for decay after irradiation. A small additional correction (~2%) for decay of the ^{24}Na during the irradiation (one hour) has been applied. Overall uncertainty in the proton beam determination by this method is about 1.8%.

As indicated in Figure 1, a third device was also used to monitor the proton beam current. This was a Bergoz Model ICT-122-070-20:1 integrating current transformer (ICT). The transformer was mounted between the beam line vacuum exit window and the pellicle used in the beam imaging system. Its signal was processed by a charge sensitive preamplifier, linear main amplifier, and analogue-to-digital converter (ADC). This device measured the charge in each micropulse of the beam and was used for real time monitoring of the proton beam at the control station for the experiment. Additionally the ADC outputs were stored in a histogram for each irradiation. The centroid of this histogram provided a measure of the average charge per beam pulse. Multiplication by the total number of beam pulses gave the integrated beam charge. This system was calibrated by recording the ADC output for the injection of a known charge into a wire loop through the ICT. Overall uncertainty of this technique was estimated to be 4%, determined mainly by the uncertainty of the injected calibration charge.

Table 2 summarizes the results for the determination of the total number of protons incident on the sample for each of the two irradiations. Note that the values from the three methods are consistent within the estimated uncertainties. The values used to normalize the irradiations were taken to be the weighted average of the values from the three methods and have an uncertainty of 1.5%.

Table 2 Results for the determination of the total proton fluence		
Measurement Technique	Sodium Sample Irradiation (protons on target)	Empty Container Irradiation (protons on target)
LAMPF current monitor (est. 4.5% uncertainty)	6.10×10^{14}	6.52×10^{14}
Aluminum foil activation (est. 1.8% uncertainty)	6.36×10^{14}	6.47×10^{14}
Integrating current transformer (est. 4% uncertainty)	6.59×10^{14}	6.83×10^{14}
Weighted Average (uncertainty 1.5 %)	**6.36×10^{14}**	**6.52×10^{14}**

The position and profile of the incident proton beam was monitored during tune-up using a phosphor screen (with a graticule) about 5 cm upstream from the sample position. This phosphor was viewed by a video imaging system (see Figure 1). In this system, the image of the phosphor screen is relayed by a pellicle (64 micron thick aluminized mylar located in the beam between the ICT and the phosphor) to a front surface mirror (located 5 meters from the beam) and thence focused by a lens onto a gated microchannel-plate intensifier coupled to a CCD camera. The signal from this camera was transmitted to a recording station where it was viewed in real time to insure proper position and focus of the beam and also recorded on a VCR for later analysis. A typical beam spot image is shown in Figure 3. Over the course of the irradiations, the size and position of the proton beam proved to be very stable and reproducible.

The footprint of the proton beam on the sample was checked with an auto-radiograph of the sample made by placing it in contact with an image storage phosphor. Figure 4 shows the results of this measurement. This radiograph indicated that the beam was centered on the sample to within about 2 mm. Line profiles through the image indicated that the bulk of the irradiated area was inside a radius of 1 cm.

The thickness of the sodium sample container over the region irradiated by the proton beam was sampled at 13 points using a micrometer. The container thickness was taken as the average over those points within 1 cm of the sample center. The uncertainty was estimated by the statistical variance of the measured points and amounted to 2.7%. The sodium thickness was calculated assuming the sodium completely filled the space between the stainless steel walls and had a density of 0.971 gms/cc.

After storage for about one week the samples were counted using a large (55% efficiency) Germanium detector. Samples were located 50 cm from the detector and were mounted in a

fixture which was attached to the detector assembly with alignment pins to insure accurately reproducible positioning. The sample counting was performed 7, 17 (two independent counts were done here), and 25 days after irradiation. This was done to verify that the peaks associated with the ^{7}Be and ^{22}Na gamma rays demonstrated the expected half-lives. A set of measurements consisted of four counting runs. These consisted of the following: 1) The sodium sample irradiated in the proton beam, 2) the sodium sample located just outside the proton beam, 3) the stainless steel can irradiated in the proton beam, and 4) the stainless steel located just outside the beam. Pulse-height spectra from the Ge detector for a measurement set are shown in Figure 5. Details in the region of the ^{7}Be and ^{22}Na gamma rays are shown in Figure 6 and 7. Note that ^{7}Be has a half-life of 53.29 days and decays by electron capture, emitting a 478 keV gamma ray with a branching ratio of 10.45%. ^{22}Na has a half-life of 2.6019 years with a 1.368 MeV gamma ray emitted in 99.935% of the decays.

Reference to Figure 5 indicates that while there are a relatively large number of gamma rays associated with the activity in the stainless steel, the gamma rays from ^{7}Be and ^{22}Na are well separated from other lines. Figure 6 shows an expanded view near the 478 keV gamma ray from ^{7}Be. While there is no significant contribution from the samples which were out of the beam, the stainless steel can does show some production of ^{7}Be. This contribution was subtracted from the data with the Na sample to arrive at the activity associated with the sodium. Figure 7 demonstrates that there is no significant contribution to the ^{22}Na gamma ray from any of the other samples. The data for this isotope were taken directly from the spectrum for the in-beam sodium sample. In both cases the measured gamma ray count rates were corrected for self-absorption in the sample and can. These corrections were small, being less than 5% for either case.

The counting rates were further corrected for dead time and pile-up losses in the detector and data acquisition system. These corrections were small, being less than 2% in all cases. The corrected count rates were converted to activity using a measured efficiency curve for the detector. This efficiency curve was determined using a series of calibrated gamma-ray sources (^{133}Ba, ^{137}Cs, ^{60}Co, ^{22}Na) and an uncalibrated source (^{152}Eu) used to check the energy-dependent relative efficiency. The uncertainty in the determined efficiency for the 478 keV gamma ray from ^{7}Be was dominated by the uncertainty in the ^{133}Ba source used for this energy region and was quoted by the supplier to be 4.8% at the 99% confidence level. Likewise for the 1.368 MeV gamma ray from ^{22}Na, the efficiency uncertainty was dominated by the uncertainty in the ^{22}Na calibration source and was quoted by the supplier to be 3.7% at the 99% confidence level. Additional uncertainties in the measured gamma ray activities came from the counting statistics and uncertainties in peak area determinations, combined for both foreground and background contributions.

The measured activities were corrected for the decay after irradiation and branching ratios and then converted to cross sections using the measured proton fluence and sample thickness. Data for the cross sections derived from the four different counts were used to form a weighted average using the statistical uncertainties associated with each separate measurement. The statistical

uncertainty on the average value was then combined with the various systematic uncertainties to produce the final overall uncertainty. The derived cross sections and their estimated total uncertainties are listed in Table 3.

Table 3
Measured Cross Sections and Uncertainties

Isotope	Cross Section (millibarns)	Uncertainty (millibarns)
^{7}Be	6.50	0.24
^{22}Na	29.45	1.00

Simulations using the MCNPX code

MCNPX (version 2.1.5) was used to model the experimental geometry. The MCNPX code (ref. 1) is a major extension of the MCNP code allowing it to track all particles at all energies. A simple model was created to simulate an 800 MeV proton beam incident on a thin sodium sample housed in a stainless steel container. The MCNPX code uses various physics models to simulate the transport and creation of particles above the limit of tabulated cross-section and reaction rate values (typically 20 MeV or 150 MeV). MCNPX was used to generate the HISTP reaction tally file for all reactions above 20 MeV. This file tracks all of the reactions, including incident particle information and resulting product particle generation. The HISTP file was then interrogated using the utility HTAPE3X to estimate the production of isotopes during irradiation. This utility generates a list of isotopes created and the creation rate (number of atoms created in the selected region based on one incident proton).

The spallation product yield is shown in Figure 8. Sixty-four different isotopes are produced (in addition to H, tritium, and alpha particles). Most of the isotopes are radioactive with very short half-lives (less than a few seconds). Na-23 shows the largest production rate. This is not uncommon because the MCNPX HISTP file tracks particle reactions of all types – including scattering reactions. Therefore, the Na-23 production rate reflects inelastic scattering reactions (n,n') and elastic scattering. Figure 9 shows the remaining products 30 minutes after irradiation. These results are more realistic to the experimental procedure since a certain delay time would exist between irradiation and gamma counting. After 30 minutes, only eight radioactive isotopes remain, with only three of these having gamma emissions (Be-7, Na-22, and Na-24). Na-23 was not included in Figure 9 to allow for a better representation of the data of interest (the radioactive isotopes).

Results

The calculated yields of isotopes were then used to determine production cross-sections. Additional MCNPX calculations were then performed to estimate production cross-sections for proton energies from 100 to 800 MeV using the standard high-energy physics model in MCNPX (Bertini without a pre-equilibrium phase). Further calculations were performed using the ISABEL and CEM high-energy physics models available in MCNPX. Results are shown in Table 4 and Figures 10 and 11.

Results indicate that the Bertini model most closely calculates the ^{7}Be production cross-section, although, the C/E is only 0.65. The ISABEL physics model is slightly better than the Bertini model for the ^{22}Na production cross-section (C/E=1.47). However, the improvement in the estimate is only about 5 percent over the Bertini model.

These results (coupled with the calculations at lower energies) indicate that additional measurements should be performed. This will allow a better determination of the ability of MCNPX to accurately predict the production rates of isotopes and to assess if there is a deficiency in the high-energy physics models within the MCNPX code. In addition, the measurement should be repeated at 800 MeV to verify the experimental results.

Table 4

MCNPX-2.1.5 Calculations of ^{7}Be and ^{22}Na Production Rates in Sodium Sample

	Proton	Be-7 Production				Na-22 Production			
High-Energy	Energy			cross-section	error			cross-section	error
Physics Model	(MeV)	(atoms/proton)	error	(barns)	(barns)	(atoms/proton)	error	(barns)	(barns)
Bertini	100	3.05E-07	0.378	2.40E-05	9.09E-06	8.52E-04	0.0072	6.71E-02	4.83E-04
	200	2.87E-06	0.1078	2.26E-04	2.43E-05	6.98E-04	0.0069	5.50E-02	3.80E-04
	300	6.43E-06	0.072	5.07E-04	3.65E-05	6.44E-04	0.0072	5.07E-02	3.65E-04
	400	1.38E-05	0.0491	1.09E-03	5.35E-05	6.32E-04	0.0073	4.97E-02	3.63E-04
	500	2.27E-05	0.0383	1.79E-03	6.86E-05	6.21E-04	0.0073	4.89E-02	3.57E-04
	600	3.67E-05	0.0302	2.89E-03	8.72E-05	6.14E-04	0.0074	4.83E-02	3.58E-04
	700	4.51E-05	0.0272	3.55E-03	9.67E-05	5.96E-04	0.0075	4.70E-02	3.52E-04
	800	5.39E-05	0.0249	4.24E-03	1.06E-04	5.77E-04	0.0076	4.54E-02	3.45E-04
Isabel	800	2.61E-05	0.0357	2.06E-03	7.34E-05	5.50E-04	0.0076	4.33E-02	3.29E-04
CEM	800	9.33E-07	0.189	7.35E-05	1.39E-05	6.35E-04	0.0073	5.00E-02	3.65E-04
Bertini Pre-equilibrium	800	5.39E-05	0.0249	4.24E-03	1.06E-04	5.77E-04	0.0076	4.54E-02	3.45E-04
Results from Measurement	800			6.50E-03	2.40E-04			2.95E-02	1.00E-03

References

1. L.S. Waters, ed. "MCNPX User's Manual, Version 2.1.5," Report TPO-E83-UG-X-00001 (November 14, 1999).
2. F. R. Gallegos, "Development of a Low Intensity Current Monitor System," Los Alamos National Laboratory report LA-UR-91-3400 (1991).

3. G. L. Morgan, K, R. Alrick, A. Saunders, F. C. Cverna, N. S. P. King, F. E. Merrill, L. S. Waters, A. S. Carroll, A. L. Hanson, R. P. Liljestrand, R. T. Thompson, E. A. Henry, "Total cross sections for production of ^{22}Na and ^{24}Na in proton-induced reactions on ^{27}Al from 0.4 to 22 GeV", to be published.

Figure Captions

1. Schematic diagram of the experimental set up showing the system used to monitor the proton beam.
2. Photograph of the sodium sample in its stainless steel can.
3. Video frame showing the proton beam spot on the phosphor screen. The tic marks seen on the screen are 1 cm apart.
4. Auto-radiograph of the sodium sample indicating the area activated by the proton beam.
5. Gamma ray spectra observed for the four samples from the irradiations. In the legend, "in" means samples that were actually in the proton beam, "out" refers to those samples located near to, but not actually in, the beam.
6. Expanded view of the gamma ray spectra in the region of the 478 keV peak.
7. Expanded view of the gamma ray spectra in the region of the 1.368 MeV peak.
8. Spallation product yield in Sodium target for 800 MeV protons.
9. Spallation product yield in Sodium target after 30 minutes for 800 MeV protons.
10. Total production cross-sections for Na-23(p,x)Be-7 reaction.
11. Total production cross-sections for Na-23(p,x)Na-22 reaction.

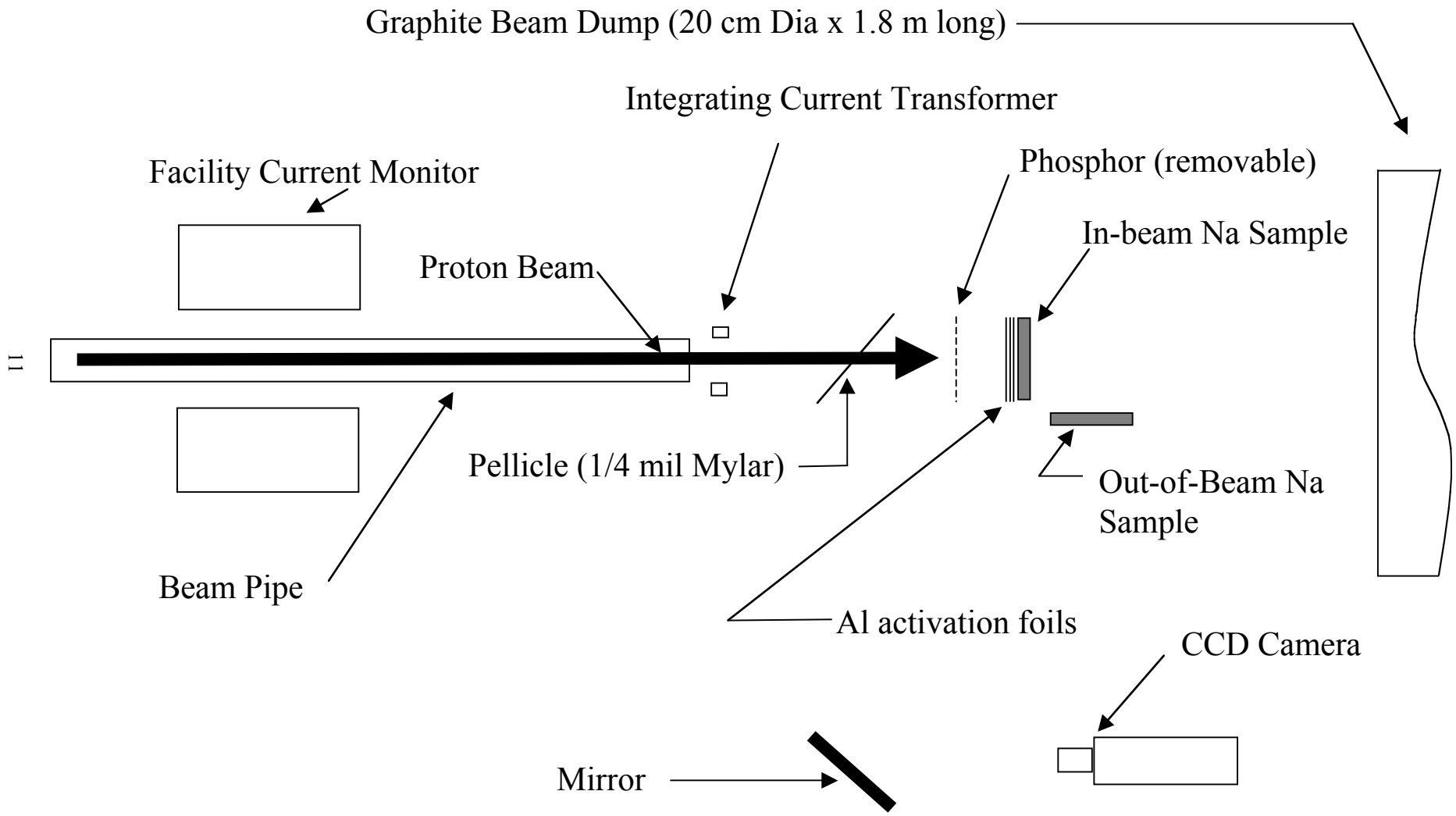
Graphite Beam Dump (20 cm Dia x 1.8 m long)
Integrating Current Transformer
Facility Current Monitor
Phosphor (removable)
In-beam Na Sample
Proton Beam
11
Pellicle (1/4 mil Mylar)
Out-of-Beam Na Sample
Beam Pipe
Al activation foils
CCD Camera
Mirror

Figure 1

Figure 2

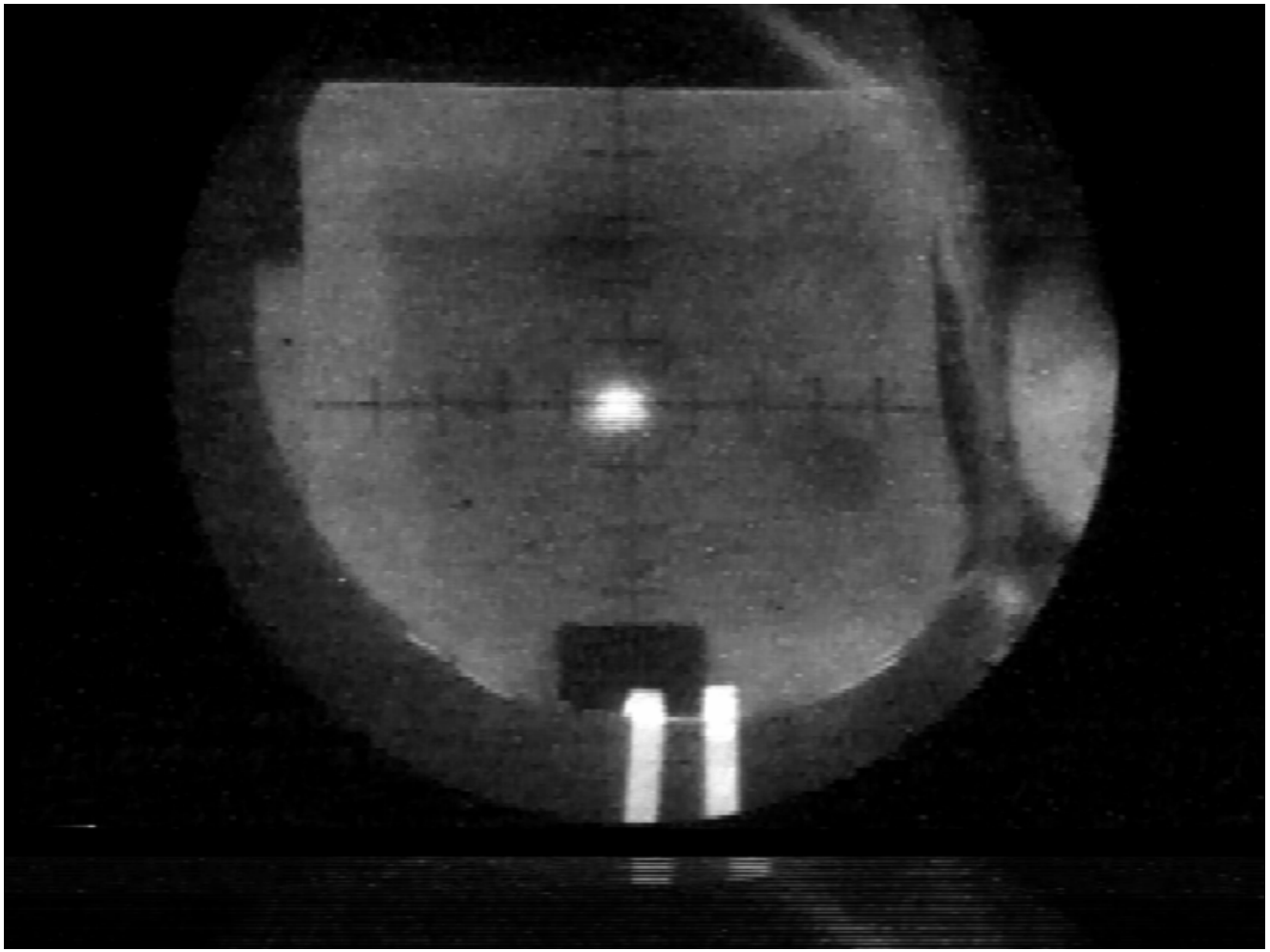

Figure 3

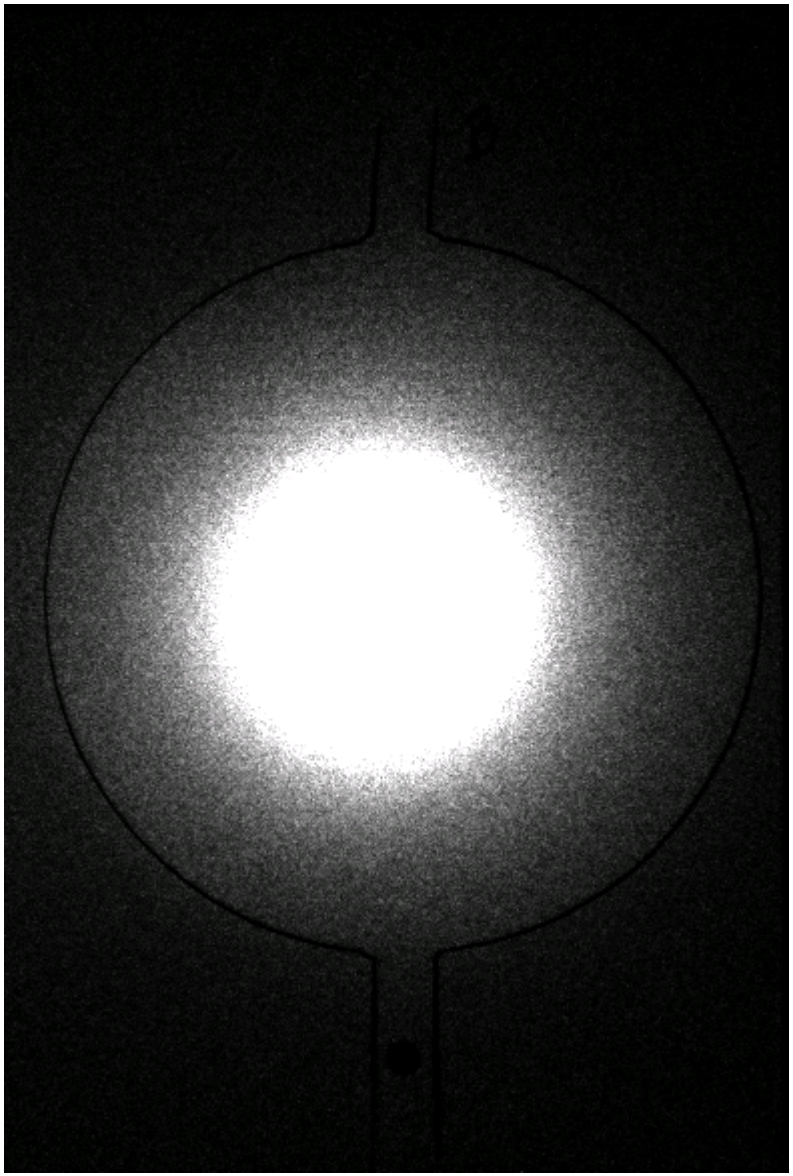

Figure 4

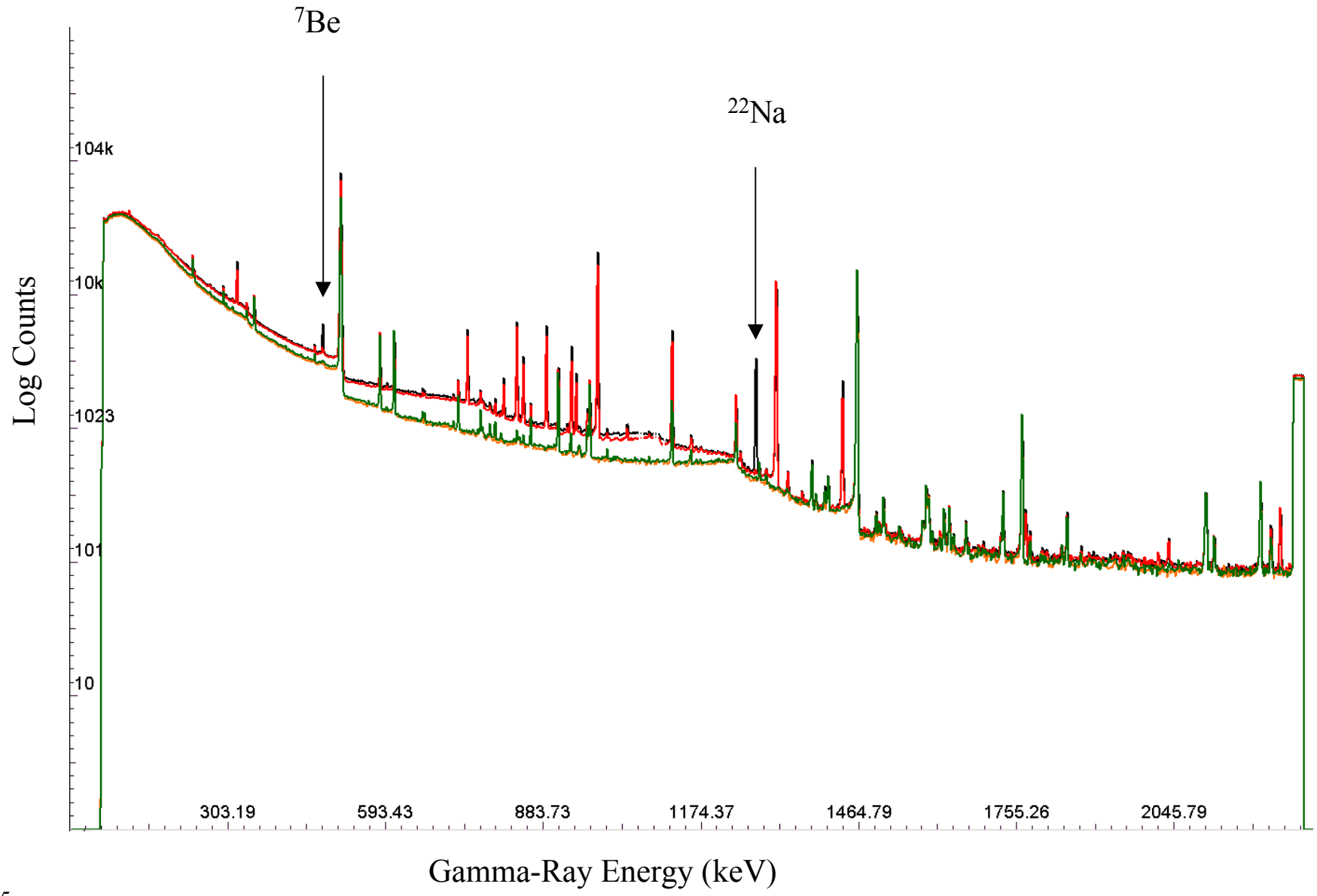
^{7}Be
^{22}Na
104k
10k
1023
101
10
Log Counts
303.19
593.43
883.73
1174.37
1464.79
1755.26
2045.79
Gamma-Ray Energy (keV)

Figure 5

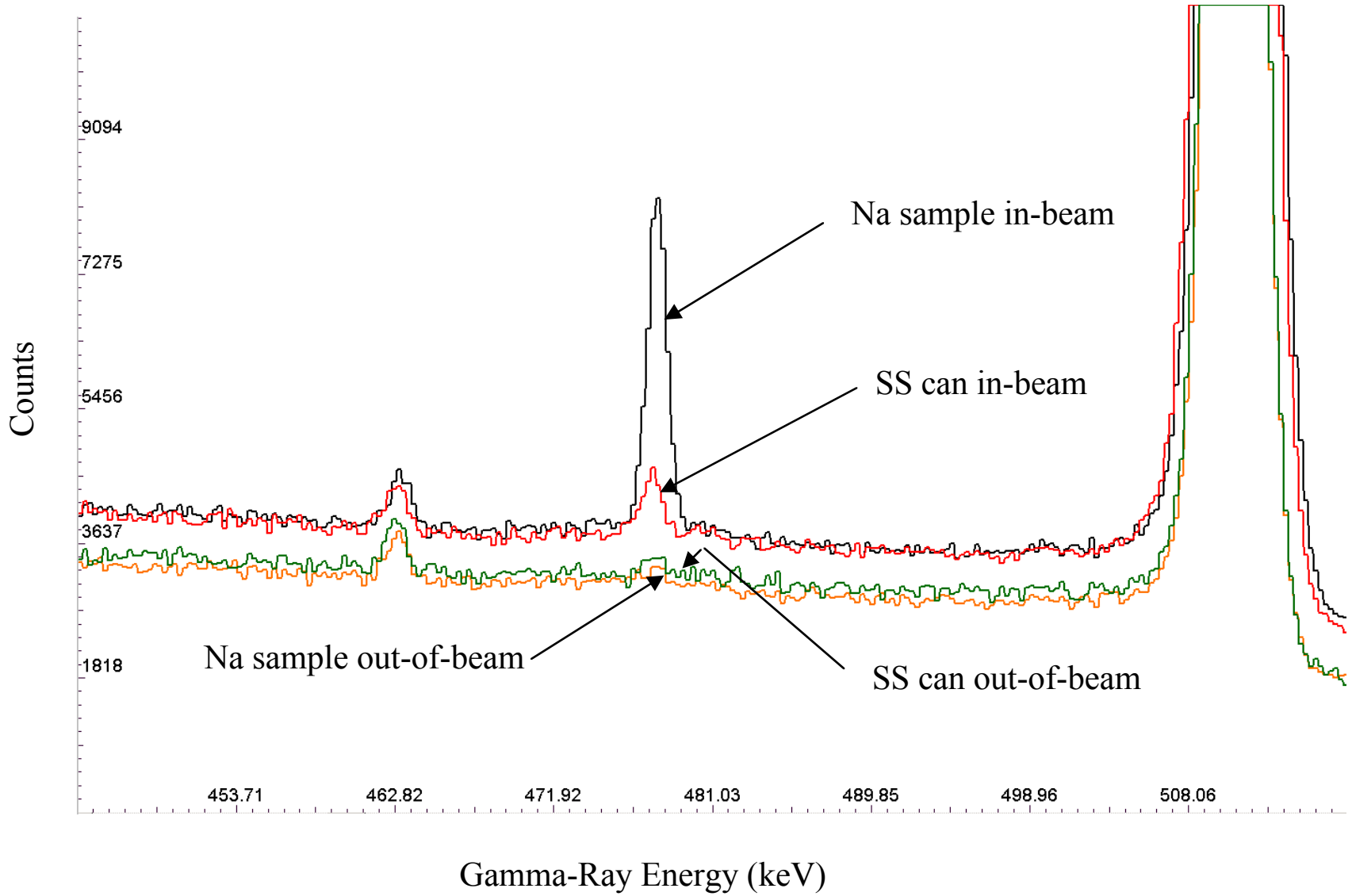
Counts
9094
7275
5456
3637
1818
Na sample in-beam
SS can in-beam
Na sample out-of-beam
SS can out-of-beam
453.71
462.82
471.92
481.03
489.85
498.96
508.06
Gamma-Ray Energy (keV)

Figure 6

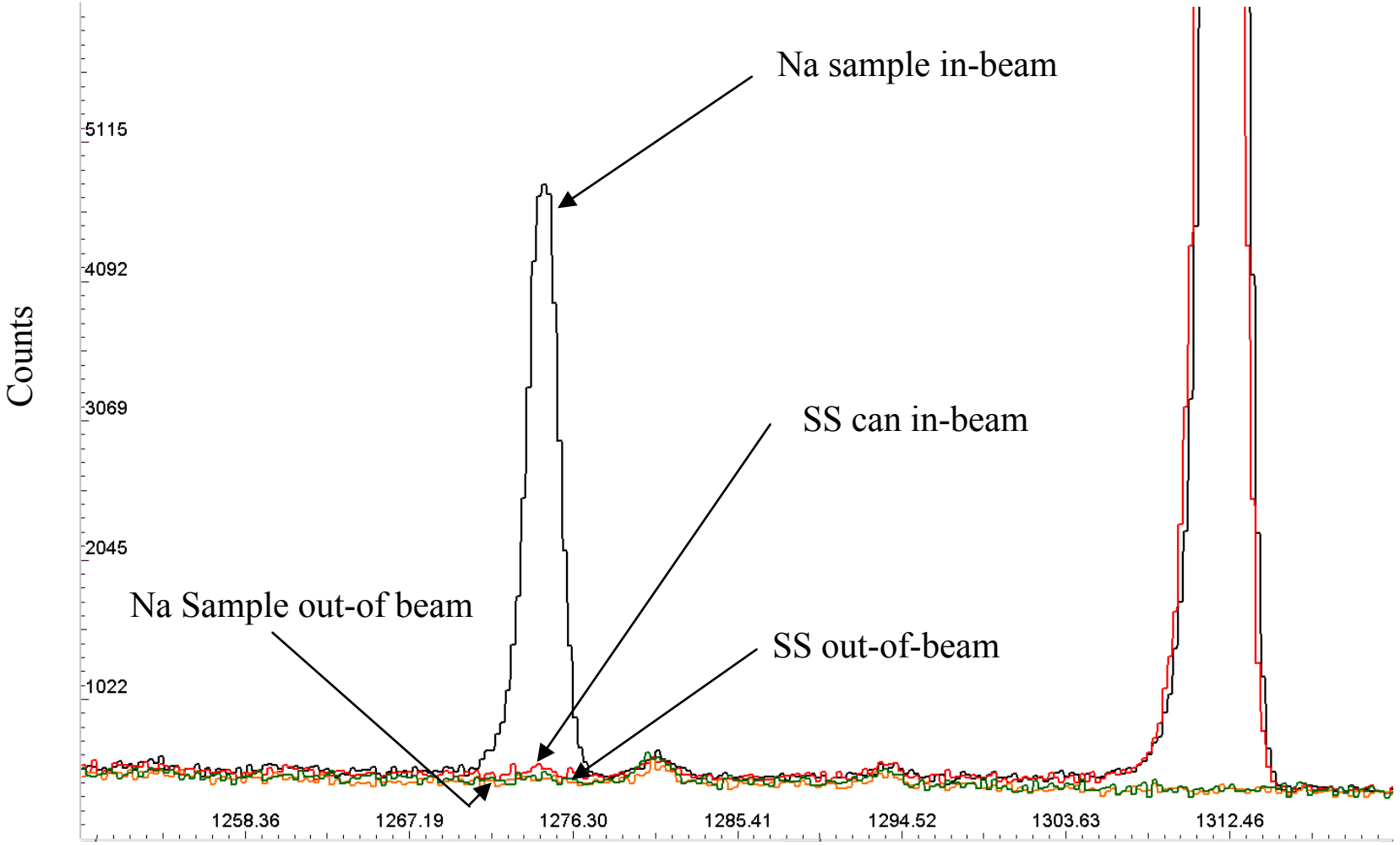
Na sample in-beam
SS can in-beam
Na Sample out-of beam
SS out-of-beam
Counts
5115
4092
3069
2045
1022
1258.36
1267.19
1276.30
1285.41
1294.52
1303.63
1312.46
Gamma-Ray Energy (keV)

Figure 7

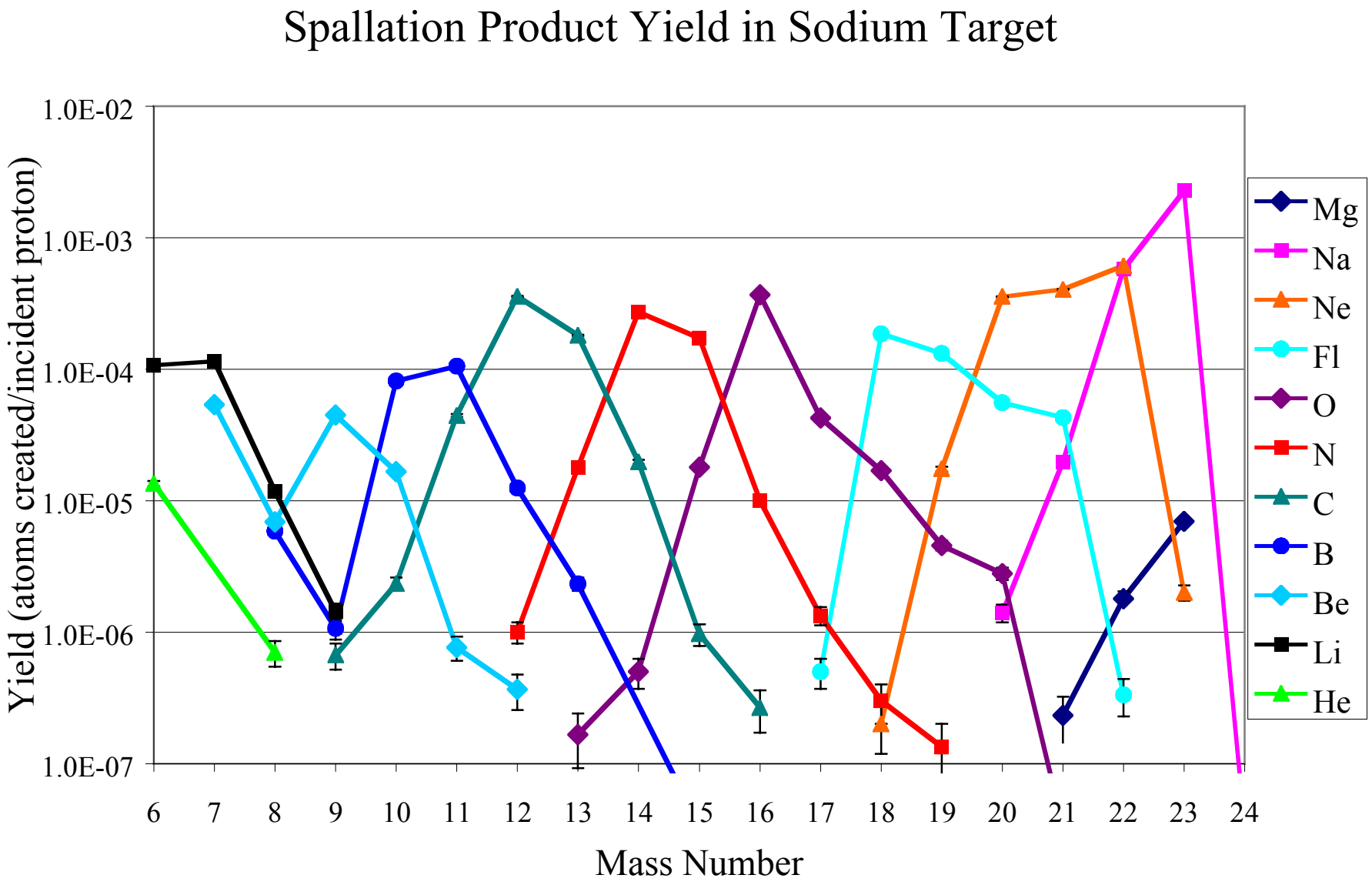
Spallation Product Yield in Sodium Target
Yield (atoms created/incident proton)
1.0E-02
1.0E-03
1.0E-04
1.0E-05
1.0E-06
1.0E-07
6
7
8
9
10
11
12
13
14
15
16
17
18
19
20
21
22
23
24
Mass Number
Mg
Na
Ne
Fl
O
N
C
B
Be
Li
He

Figure 8

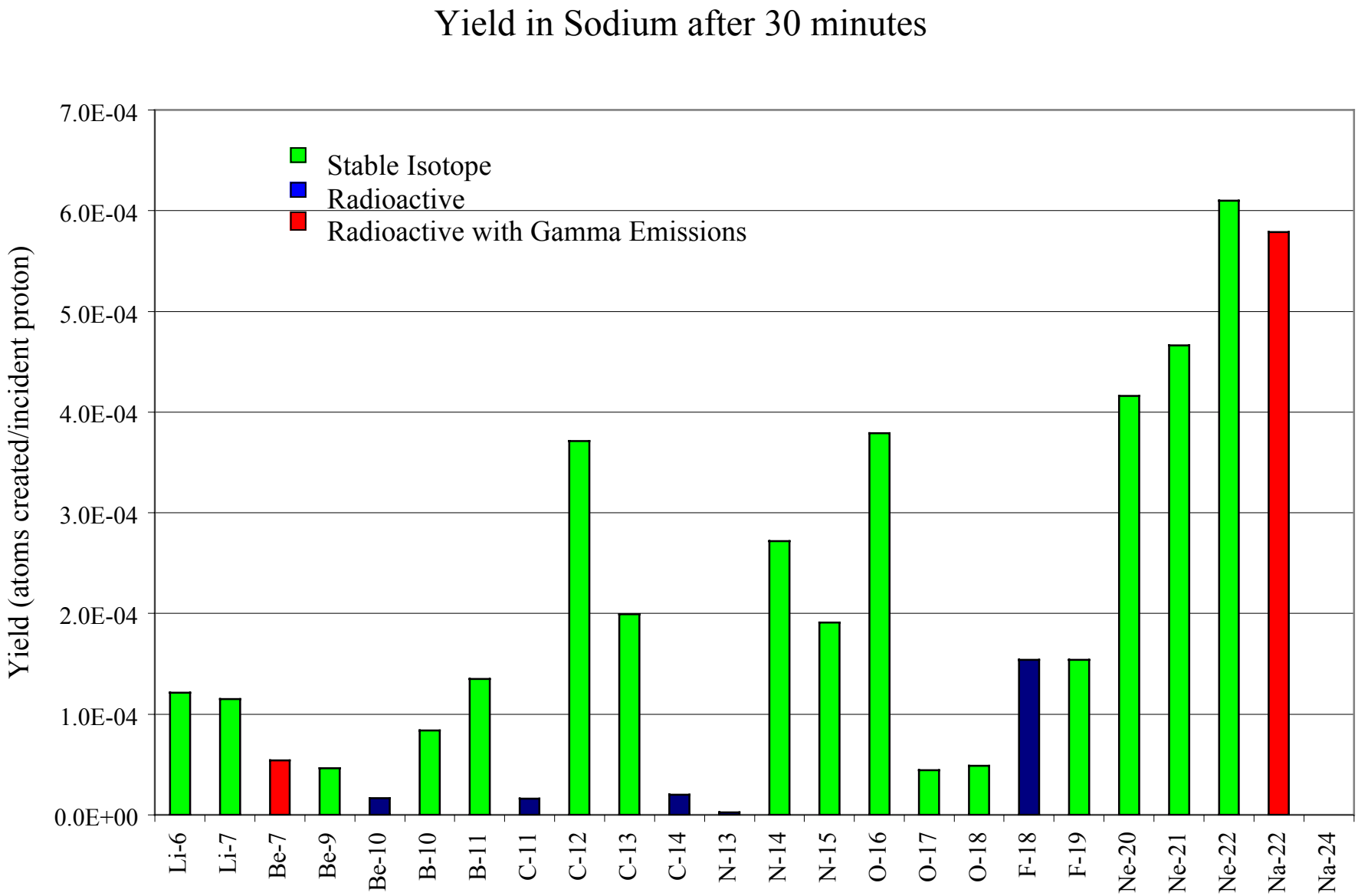
Yield in Sodium after 30 minutes
Yield (atoms created/incident proton)
7.0E-04
6.0E-04
5.0E-04
4.0E-04
3.0E-04
2.0E-04
1.0E-04
0.0E+00
Stable Isotope
Radioactive
Radioactive with Gamma Emissions
Li-6
Li-7
Be-7
Be-9
Be-10
B-10
B-11
C-11
C-12
C-13
C-14
N-13
N-14
N-15
O-16
O-17
O-18
F-18
F-19
Ne-20
Ne-21
Ne-22
Na-22
Na-24

Figure 9

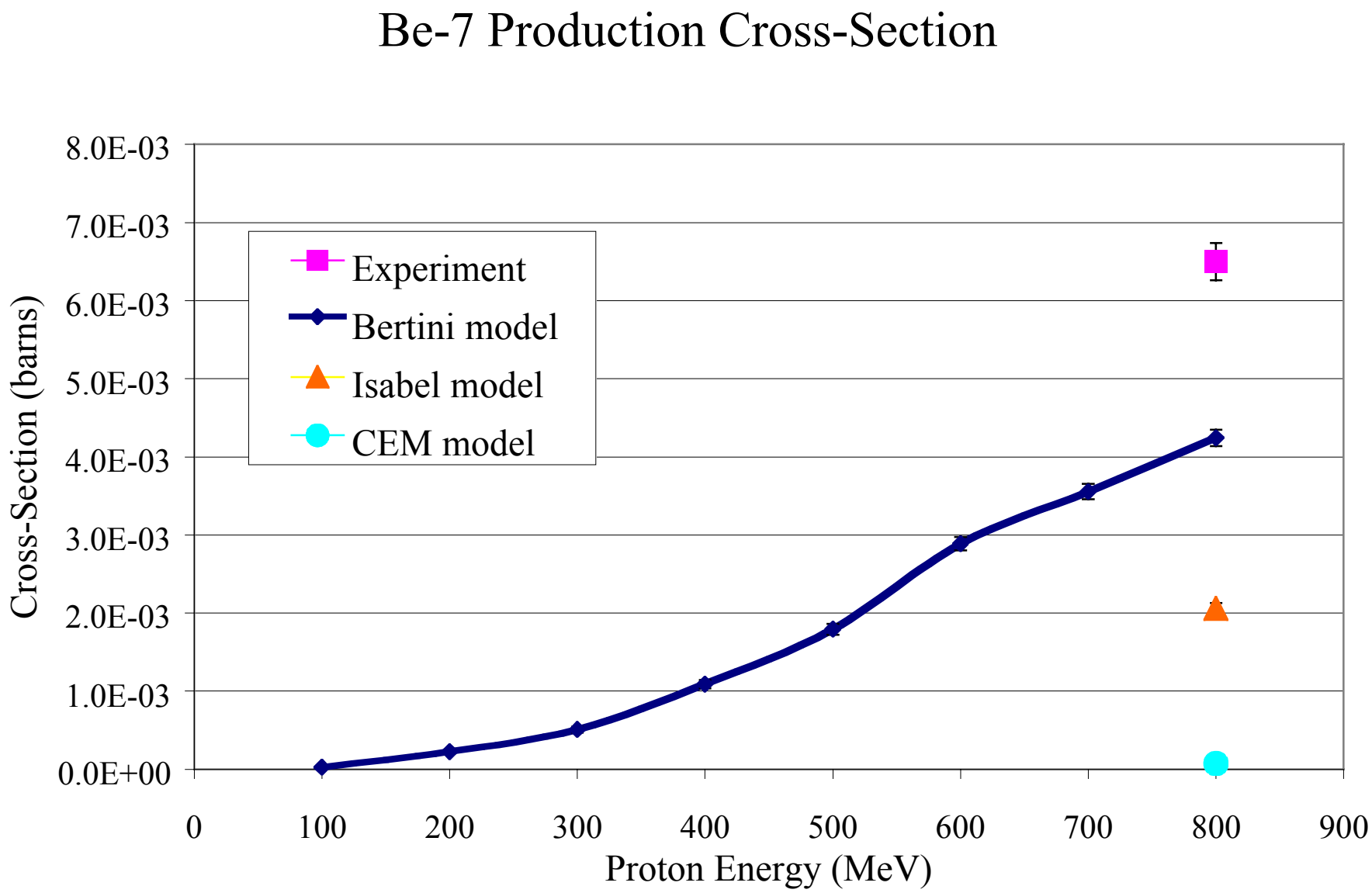
Be-7 Production Cross-Section
8.0E-03
7.0E-03
6.0E-03
5.0E-03
4.0E-03
3.0E-03
2.0E-03
1.0E-03
0.0E+00
Cross-Section (barns)
Experiment
Bertini model
Isabel model
CEM model
0
100
200
300
400
500
600
700
800
900
Proton Energy (MeV)

Figure 10

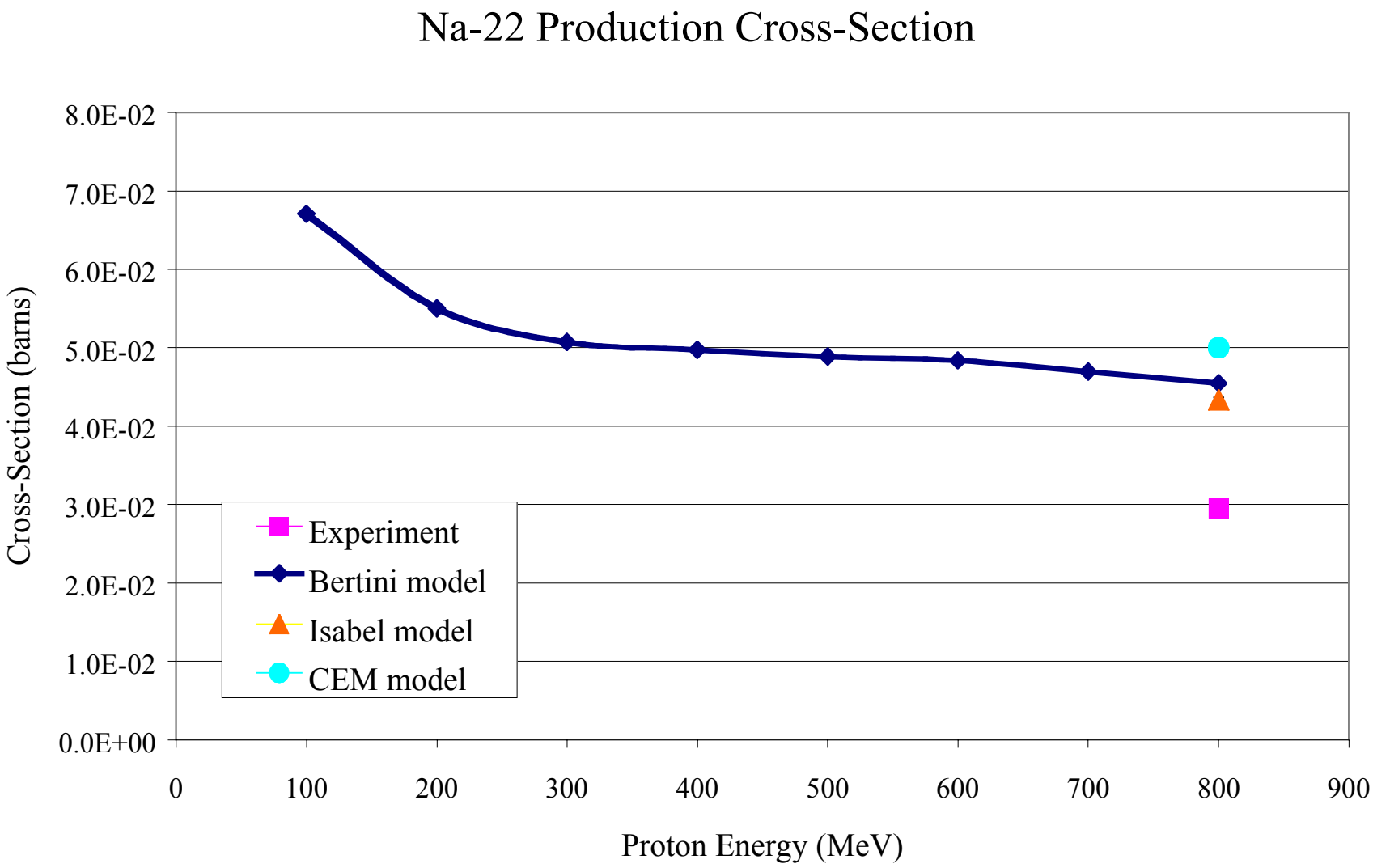
Na-22 Production Cross-Section
Cross-Section (barns)
8.0E-02
7.0E-02
6.0E-02
5.0E-02
4.0E-02
3.0E-02
2.0E-02
1.0E-02
0.0E+00
0
100
200
300
400
500
600
700
800
900
Proton Energy (MeV)
Experiment
Bertini model
Isabel model
CEM model

Figure 11

Los Alamos NM 87545